Open access • Journal Article • DOI:10.1051/RPHYSAP:01988002304062500

On constitutive equations for various diffusion-controlled creep mechanisms

Oscar Antonio Ruano, Oleg D. Sherby

Institutions: Spanish National Research Council, Stanford University

Published on: 01 Apr 1988

On constitutive equations for various diffusion-controlled creep mechanisms

O.A. Ruano, O.D. Sherby

Revue Phys. Appl. **23** (1988) 625-637 AVRIL **1988**, PAGE 625
Classification
Physics Abstracts
62.20H – 81.40L

On constitutive equations for various diffusion-controlled creep mechanisms

O.A. Ruano and O.D. Sherby(*)

Centro Nacional de Investigaciones Metalúrgicas, CSIC, Avenida Gregorio del Amo 8, 28040 Madrid Spain

(*)Department of Materials Science and Engineering, Stanford University, Stanford, CA 94305, U.S.A.

(*Reçu le 15 juin 1987, révisé le 13 janvier 1988, accepté le 14 février 1988*)

Résumé. - L'écoulement plastique des solides polycristallins à hautes températures a lieu par l'un des trois mécanismes indépendants de déformation : glissement des dislocations, glissement des joints de grain, et flux diffusionnel directionnel. On considère que les trois mécanismes sont activés thermiquement et controlés par la diffusion des atomes. On a developpé des équations constitutives qui décrivent exactement chacun des trois mécanismes indépendants. Ces équations se fondent sur une dépendence exponentielle de la vitesse de déformation. Ainsi, on montre que l'exposant de la contrainte, n, en $\varepsilon \alpha \sigma^n$, a des valeurs discrètes dépendant du mécanisme de l'écoulement plastique. Pour la déformation par glissement des dislocations, n prend des valeurs dans l'intervalle n=1 et n=8 en dépendant du mécanisme spécifique. Pour le glissement des joints de grain, n, peut-être plutôt 2 ou 4, et pour le fluage-diffusion, n est l'unité. La microstructure est un facteur important pour l'établissement de la magnitude de la vitesse de déformation dans chacun des trois mécanismes indépendants de déformation. La taille des grains est la principale caractéristique de détermination de la vitesse de déformation par le glissement des joints de grains et par le fluage-diffusion. D'autre part, la taille des sous-grains et la densité des dislocations, jouent un important rôle dans la détermination de la vitesse de déformation par le mouvement des dislocations. On montre des exemples pour des alliages ODS. Une compétition entre ces différents mécanismes peut être décrite quantitativement par l'usage des équations constitutives et des cartes de mécanismes de déformation. On montre que le fluage-diffusion n'est pas un processus dominant, comme on considère dans la littérature, et que le glissement des joints de grains, ou la déformation Harper-Dorn sont les mécanismes les plus probables qui ont lieu à faibles contraintes, et hautes températures pour matériaux avec taille de grain fin.

Abstract.- Plastic flow of polycrystalline solids at elevated temperatures occurs by one of three independent deformation mechanisms: slip by dislocation movement, sliding of adjacent grains along grain boundaries, and directional diffusional flow. All three mechanisms are considered to be thermally activated and controlled by the diffusion of atoms. Constitutive equations have been developed which accurately describe each of the three independent mechanisms. These equations center on a power law dependence of the creep rate. Thus the stress exponent, n, in $\dot{\varepsilon} \alpha \sigma^n$, is shown to have discrete values depending on the plastic flow mechanism. For deformation by slip, n can take on values ranging from n=1 to n=8 depending on the specific dislocation mechanism. For grain boundary sliding, n can be either 2 or 4, and for diffusional creep, n is unity. The microstructure is an important factor in establishing the magnitude of the creep rate for each of the three independent deformation mechanisms. Grain size is the principal microstructural feature in determining the creep rate for deformation by grain boundary sliding and by diffusional flow. On the other hand, the subgrain size and the dislocation density plays an important role in determining the creep rate for deformation by dislocation motion; examples are shown for ODS alloys. Competition between these various mechanisms can be described quantitatively through the use of constitutive equations and deformation mechanism maps. It is shown that diffusional creep is not as dominating a process as has been considered in the literature, and that grain boundary sliding or Harper-Dorn creep are the more likely deformation mechanisms occurring at low stresses and high temperatures for fine grain size materials.

1. Introduction

In the last thirty years much experimental effort has been expended to understanding creep deformation of polycrystalline materials at elevated temperatures. Usually the data are obtained from uniaxial tests of either two classes: i) creep tests where a dead-load is applied to the sample through a lever arm and its length is measured as a function of time or ii) constant strain-rate tests where the sample, held between two grips, is deformed at a constant crosshead-speed and the exerted force is measured as a function of time.

In order to determine the possible controlling mechanisms, the experimental data are compared with proposed mechanisms of deformation. Usually,

the association of the activation energy for creep with that for lattice self-diffusion or grain boundary diffusion is considered in most of the deformation models.

In a general form, the creep rate or strain rate, $\dot{\varepsilon}$, has been observed to be related with the absolute temperature, T:

$$\dot{\varepsilon} = f(s) \exp(-Q/RT) (\sigma/E)^n \qquad (1)$$

where

f(s) = function of structure,
E = average unrelaxed polycrystalline Young's modulus,
n = stress exponent,
Q = activation energy for plastic flow,
R = universal gas constant.

The function f(s) represents principally the influence of grain size, d, subgrain size, λ, and dislocation density, ρ. Over a certain temperature range, Q is constant and is related to a particular deformation mechanism.

Although time-dependent deformation of metals at high temperatures, above 0.6 T_m (where T_m is the absolute melting temperature), is usually correctly described by a diffusion-controlled dislocation creep mechanism, other mechanisms may become important. Grain boundary sliding and directional diffusional flow may in fact dominate deformation especially in fine-grained materials. These three mechanisms are considered to operate independently of one another, are thermally activated, are controlled by atom diffusion and can be described by Eq. (1).

Each of the mechanisms for creep has specific values of n and Q by which the mechanism can be defined uniquely. For example, plastic flow by slip is associated with a high stress exponent (5 or higher) and an activation energy equal to that for lattice self-diffusion, Q_L. Plastic deformation by grain boundary sliding is characterized by a low stress exponent of about 2 and an activation energy which is equal to Q_L or to the activation energy for grain-boundary diffusion, Q_{gb}. Plastic deformation by diffusional flow is characterized by a stress exponent of unity and an activation energy equal to Q_L or Q_{gb}.

As mentioned, deformation at high temperatures is dominated by the effects of diffusion controlled creep which allows the attainment of a steady state. The existing deformation mechanism models, in general, describe well the steady state creep properties and permit accurate predictions of the deformation behavior. At intermediate temperatures, however, in the range (0.3-0.6) T_m, the measured activation energies for creep are usually smaller than those for lattice self-diffusion. In this range, basically two approaches has been taken:

1) Description of the deformation behavior involving the contribution of pipe diffusion to the overall atom mobility, if a steady state can be reached.

2) Description of the deformation behavior by thermally activated cross slip [1,2], intersection of moving dislocations with dislocation forests [3], interaction of dislocations with impurity atoms [4] and dislocation glide controlled by the Peierls stress [5].

Much controversy still exists on the controlling creep mechanisms at intermediate temperatures because any mechanism satisfactorily explains the experimental creep data for a large number of materials. In the present review only diffusion controlled creep will be considered.

2. Deformation mechanisms

Three principal modes of deformation, as mentioned, have generally been considered in explaining the creep behavior of polycrystalline materials, namely diffusional flow, grain boundary sliding (GBS) and slip creep. Each of these mechanisms can be described by a constitutive equation of the form of Eq. (1). If only the influence of grain size on the function f(s) is considered, the following creep equation can be used:

$$\dot{\varepsilon} = A (b/d)^p D_{eff} (Eb^3/kT)^q (\sigma/E)^n \qquad (1a)$$

where A, n, q and p are material constants, b is Burgers' vector and D_{eff} is the effective diffusion coefficient as is given by

$$D_{eff} = D_L f_L + D_p f_p + D_{gb} f_{gb} \qquad (2)$$

where D_L, D_p and D_{gb} are the lattice, dislocation pipe diffusion and grain boundary diffusion coefficients respectively, and f_L, f_p and f_{gb} are the fractions of atoms participating in lattice, pipe and grain boundary diffusion respectively. This means that, in a general sense, the presence of dislocations within the lattice makes it necessary to include the contribution of pipe diffusion to the overall atom mobility [6,7].

Table I resumes the constitutive equations for creep corresponding to the three mentioned modes of deformation of polycrystalline metals.

Diffusional creep

Diffusional creep is based on the redistribution of vacancy concentrations in the vicinity of grain boundaries which are subjected to normal stresses. When a vacancy is formed at a grain boundary that is

Table I. Constitutive equations for creep of polycrystalline metals of high stacking fault energy.

Creep process	Eq.*	Equation
Diffusional flow		
Nabarro-Herring	(3)	$\dot{\varepsilon} = 14 (D_L/d^2) (E b^3/k T) (\sigma/E)$
Coble	(4)	$\dot{\varepsilon} = 50 (D_{gb} b/d^3) (E b^3/k T) (\sigma/E)$
Boundary sliding		
Lattice diffusion controlled	(5)	$\dot{\varepsilon} = 6.4 \times 10^9 (D_L/d^2) (\sigma/E)^2$
Grain boundary diff. contr.	(6)	$\dot{\varepsilon} = 5.6 \times 10^8 (D_{gb} b/d^3) (\sigma/E)^2$
Slip		
Lattice diffusion controlled	(7)	$\dot{\varepsilon} = 10^{11} (D_L/b^2) (\sigma/E)^5$

subjected to a normal tensile stress, σ_1, a force that is equal to $\sigma_1 b^2$ will move the vacancy a distance b. The required energy to create a vacancy in this region is reduced by the amount $\sigma_1 \Omega$ where Ω is the atomic volume. A flux of vacancies through the lattice, given by Fick's law, may then exist from those boundaries subjected to tension to those subjected to compression. The equation, obtained independently by Nabarro [8] and Herring [9], has n=1, p=2, q=1 and $Q=Q_L$. Constant A depend on the grain boundary shape, but has a typical value of 14.

For the flux of vacancies taking place along grain boundaries, Coble [10] calculated the creep rate to have n=1, p=3, q=1 and $Q=Q_{gb}$. Constant A for this case is about 50.

The specific equations for Nabarro-Herring and Coble creep are shown as Eqs. (3) and (4) (Table I) respectively.

Grain boundary sliding

Grain boundary sliding occurs by the movement of individual grains sliding over each other along their common boundary. The most important phenomenon that may result from grain boundary sliding is the enhanced ductility, or superplasticity, associated with fine grains which remain essentially equiaxed after deformation. Observations made on

Table II. Summary of proposed models of grain boundary sliding.

Mechanism	Creep Equation	Ref.	Remarks
Diffusional Accomodation (rate controlling)			
Ashby-Verrall	$\dot{\varepsilon} = K_1 (b/d)^2 D_{eff} (\sigma - \sigma_0/E)$	12	$D_{eff} = D_L [1 + (3.3w/d)(D_{gb}/D_L)]$
Slip Accommodation (rate controlling)			
Ball-Hutchison	$\dot{\varepsilon} = K_2 (b/d)^2 D_{gb} (\sigma/E)^2$	13	Slide of group of grains
Mukherjee	$\dot{\varepsilon} = K_3 (b/d)^2 D_{gb} (\sigma/E)^2$	14	Grains slide individually
Gifkins	$\dot{\varepsilon} = K_4 (b/d)^2 D_{gb} (\sigma/E)^2$	15	Pile up at triple points(core-mantle)
Langdon	$\dot{\varepsilon} = K_5 (b/d) D_L (\sigma/E)^2$	16	Movement of dislocations adjacent to g.b.
Gittus	$\dot{\varepsilon} = K_6 (b/d)^2 D_{IPB} (\sigma - \sigma_0/E)^2$	17	Pile up at interphase boundary (IPB)
Hayden et al.	$\dot{\varepsilon} = K_7 (b/d)^3 D_p (\sigma/E)^2$	18	$T < T_c$ GBS is rate controlled by slip
	$\dot{\varepsilon} = K_7 (b/d)^2 D_L (\sigma/E)^2$		$T > T_c$ creep in the grains
Arieli-Mukherjee	$\dot{\varepsilon} = K_8 (b/d)^2 D_{gb} (\sigma/E)^2$	19	Climb of individual dislocations near g.b.
Diffusional Accommodation (not rate controlling)			
Padmanabhan	$\dot{\varepsilon} = K_9 (b/d)^2 D (\sigma/E)^2$	20	D may differ from D_L and D_{gb}

Definitions: K_1 - K_9 = material constants, σ_0 = threshold stress, w = grain boundary width, T_c = critical temperature.

superplastic materials revealed that individual grain rotate and switch neighbors while sliding over each other [11]. No gross formation of cavities is observed under optimal deformation conditions. In order for the grains to mantain compatibility during the deformation process an accommodation process is incorporated which avoid the formation of holes at triple junctions. This accommodation process is interdependent with the process of GBS and the slower will be rate controlling.

Several deformation mechanisms have been proposed to describe GBS. Table II summarizes the creep equations that have been developed by different models [refs. 12-20]. The deformation can be controlled by the grain boundary itself or by the accommodation process. This may take place by diffusional flow or by slip. As can be seen, the models have n=2 (except for the Ashby-Verrall model), p=1 to 3, q=0 and $Q=Q_L$ or Q_{gb}.

An examination of experimental data for a large number of materials deformed by GBS revealed that none of the proposed equations are consistent with these data. For this reason, a phenomenological flow stress-strain rate relationship was developed to best fit the avilable experimental data. Such phenomenological analysis used n=2, q=0 and a temperature dependence of the strain rate associated either with the activation energy for lattice or grain boundary diffusion [21]. Those materials where the creep rate is controlled by lattice diffusivity showed p=2. Those materials where the creep rate appears to be controlled by grain boundary diffusivity showed p=3. These observations are contained in the phenomenological relations [22], Eqs. (5) and (6), given in Table I.

An example of the predictive ability of Eq. (5) in describing superplastic flow in materials where $Q=Q_{gb}$ is shown in Fig. 1 for 30 separate investigations [13,18,21,23-49]. The predicted curve from Eq. (5) is shown by the dashed line. As can be seen, the lines shown for the many materials investigated exhibit stress exponents of about two in agreement with Eq. (5). In addition, the absolute values of the creep rate, after compensation for temperature and linear intercept grain size, $\bar{L}$, are mostly within an order of magnitude of that predicted by Eq. (5) at a given value of modulus compensated stress. The relation between $\bar{L}$ and d was shown to be $d=1.776\,\bar{L}$ [50].

Similarly, Fig. 2 shows the predictive ability of Eq. (6) in describing superplastic flow in materials when $Q=Q_L$ for 17 separate investigations [18,29, 51-65]. The curve from Eq. (6), shown by the dashed line, predict well the creep behavior within an order of magnitude.

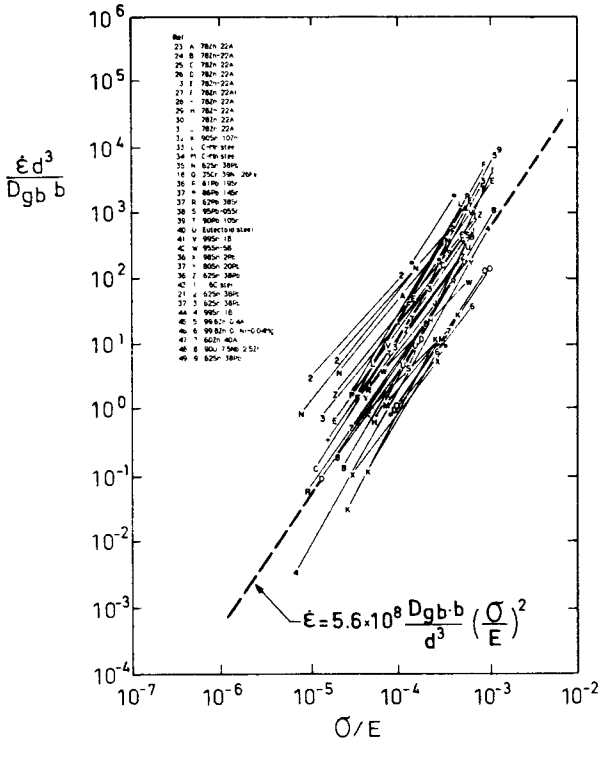

Fig. 1. Diffusion- and grain-size-compensated strain rate as a function of modulus- compensated stress for polycrystalline materials where superplastic flow is controlled by grain boundary diffusion.

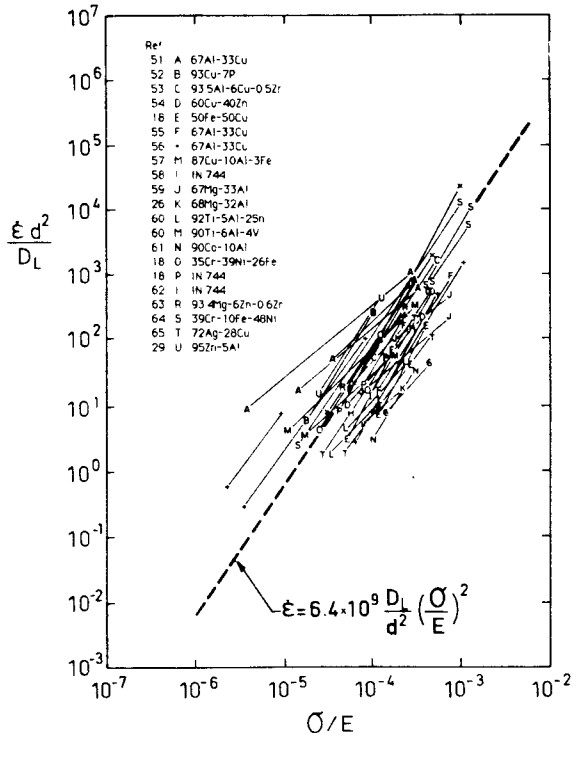

Fig. 2. Diffusion- and grain-size-compensated strain rate as a function of modulus- compensated stress for polycrystalline materials where superplastic flow is controlled by lattice diffusion.

Slip creep

The steady state creep rates for a large number of polycrystalline pure metals tested at high temperature have been observed to be associated with n=5, q=p=0 and $Q=Q_L$ [66-69]. The specific constitutive equation for describing this mode of creep, known as power-law creep, is given by Eq. (7) in Table I.

The phenomenological correlation of Eq. (7) is supported by many theoretical models. The best known is based on a dislocation climb mechanism and was proposed by Weertman [70]. In this model, dislocations are produced by symmetrically spaced Frank-Read sources in which the rate controlling process is the climb of edge dislocations from piled-up groups. Barrett and Nix [71] proposed a model based on the diffusion controlled motion of jogged screw dislocations in which the only undetermined parameter was the distance between jogs.

Some coarse-grained polycrystalline materials tested at high temperatures and low stresses show Newtonian viscous behavior (n=1) known as Harper-Dorn creep [72]. The scarcity of data has limited the number of detailed analysis of this mode of creep. It is well established, however, that the mechanism of deformation in Harper-Dorn (H-D) creep is diffusion controlled dislocation motion and that no grain size dependence exists. The phenomenological relationships correlating the existing data will be reviewed later.

3. Microstructural factors affecting the creep mechanisms.

It is well established that microstructural factors, such as subgrains and dislocation density within subgrains or grains, influence the creep rate. They may influence the creep rate by changing the rate of atom mobility (diffusion coefficient) through pipe diffusion, by serving as barriers to plastic flow (for example through the presence of subgrains) and by contributing to enhanced dislocation glide through internal stresses from non-mobile dislocations.

Pipe diffusion

As mentioned before, pipe diffusion can be important in a number of creep mechanisms, including slip creep, grain boundary sliding and even diffusional flow.

In Eq. (2), the term

$$f_p = (n / N)\,\rho \qquad (8)$$

where n = number of atoms surrounding the dislocation core, N= number of atoms per unit area and ρ = dislocation density. The dislocation density can be expressed, using the Taylor relation, as equal to $C/b^2\,(\sigma/E)^2$, where C is a constant typically equal to 5-100 [73,74]. The term $f_L=1-f_p$ is about unity. Therefore, utilizing C=50 and substituting these terms in Eq. (2):

$$D_{eff} = D_L + 50\,D_p\,(\sigma/E)^2 \qquad (9)$$

We can now substitute D_{eff} for D_L in Eqs. (3), (5) and (7) of Table I in order to have three new equations for diffusional flow, grain boundary sliding and slip creep respectively. At low stresses the term containing D_p is small compared with D_L. At high stresses, however, these equations can be written as:

$$\dot{\epsilon}_{diff} = 700\,(D_p/d^2)\,(E\,b^3/k\,T)\,(\sigma/E)^3 \qquad (10)$$

$$\dot{\epsilon}_{gbs} = 3.2 \times 10^{11}\,(D_p/d^2)\quad(\sigma/E)^4 \qquad (11)$$

$$\dot{\epsilon}_{slip} = 5.0 \times 10^{12}\,(D_p/b^2)\quad(\sigma/E)^7 \qquad (12)$$

From these equations, only Eq. (12) has been used extensively [75]. In the following, examples are gives of the predictive ability of Eq. (11)

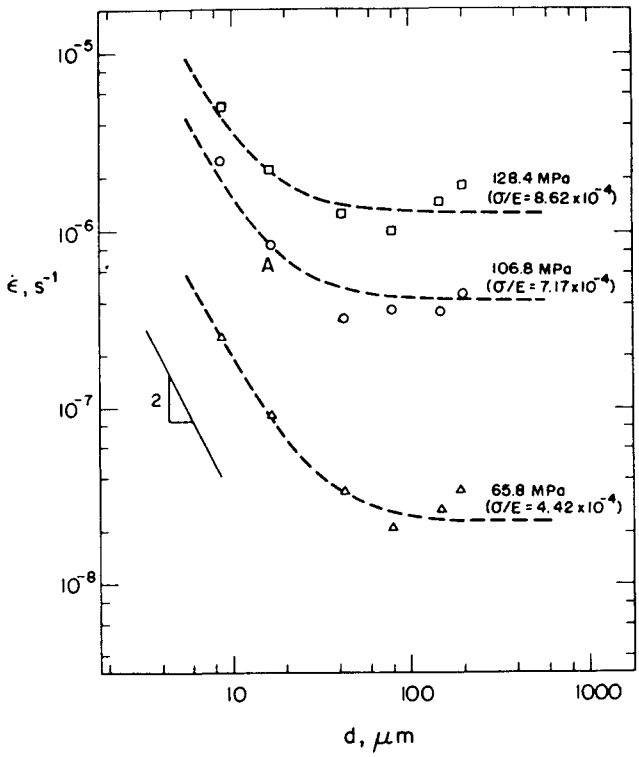

Fig. 3. The influence of grain size on the creep rate of a 17Cr-14Ni austenitic stainless steel at 704°C. The broken lines are predicted from Eq. (15).

When pipe diffusion is considered, some experimental observations which show a grain size dependence of the creep rate and a relatively large stress exponent can be explained on the basis of pipe-diffusion-controlled grain boundary sliding represented by Eq. (11).

Garofalo et al. [76] studied the effect of grain size on the creep resistance of an austenitic iron-base alloy. They showed that the grain size affected the creep rate for fine grain sizes (following the form $\dot{\epsilon} \propto d^{-2}$) but that there was no grain size effect for coarse grain sizes. This observation is illustrated in Fig. 3. Garofalo et al. explained the trend observed on the basis of grain boundaries which acted as generators of dislocations. However, they made no quantitative analysis.

The data of Garofalo et al. reveal that the stress exponent n is 4 for fine grain sizes where the creep rate was found to be proportional to d^{-2}, and the stress exponent is about 6 for coarse grain sizes. These observations indicate that the data can be analyzed in terms of pipe-diffusion-controlled grain boundary sliding, using Eq. (11), where $\dot{\epsilon} \propto \sigma^4/d^2$, and Eq. (12), where $\dot{\epsilon} \propto \sigma^7$.

The concept utilized in our analysis is that the two processes contribute to the total creep rate $\dot{\epsilon}_T$ additively. Thus

$$\dot{\epsilon}_T = \dot{\epsilon}_{gbs(Dp)} + \dot{\epsilon}_{slip} \qquad (13)$$

The term $\dot{\epsilon}_{gbs(Dp)}$ is given by Eq. (11) where only the D_p term is unknown. The term $\dot{\epsilon}_{slip}$ can readily be evaluated by analysis of the creep rate-stress relation at coarse grain sizes where slip dominates the deformation process and is done elsewhere [7]. The best fit correlation obtained in the power law range is given by

$$\dot{\epsilon} = 3.4 \times 10^{12} (\sigma/E)^6 \ s^{-1} \qquad (14)$$

Substituting Eqs. (11) and (14) into Eq. (13), it is obtained:

$$\dot{\epsilon} = 3.2 \times 10^{11} (D_p/d^2)(\sigma/E)^4 + 3.4 \times 10^{12} (\sigma/E)^6 \ s^{-1} \qquad (15)$$

Equation (15) predicts the steady state creep rate of austenitic stainless steel as a function of grain size and modulus-compensated stres at 704°C, provided that D_p is known. The value of D_p was chosen so that the $\dot{\epsilon}_T$ values fit the experimental data at a grain size of d= 17 μm at $\sigma/E = 7.17 \times 10^{-4}$. A value of $D_p = 1.4 \times 10^{-15}$ m^2 s^{-1} was used. The resulting creep rate-grain size relationship from Eq. (15) is given by the broken lines in Fig. 3. The predicted behavior agrees remarkably well with the experimental data, attesting to the validity of Eq. (15). The creep rate power dependence of 2 on the grain size together with the creep rate power dependence of 4 on the modulus-compensated stress is well verified by the experimental data in the range of fine grain sizes. These predictions give considerable support to the concept that pipe diffusion plays an important role in controlling creep when grain boundary sliding dominates.

The creep of fine-grained materials exhibits different rate-controlling regimes. Thus materials that exhibit superplastic characteristics with n=2 can be expected to show a stress exponent of n=4 as the stress is increased. An example from the literature is a fine-grained copper-base alloy investigated by Shei and Langdon [77]. Figure 4 shows the creep rate as a function of stress for this alloy. The broken lines represent the predicted behavior considering the three contributions to creep associated with GBS-D_{gb} controlled, GBS-D_p controlled and slip creep D_p controlled. Specifically, the following equation was used to correlate the

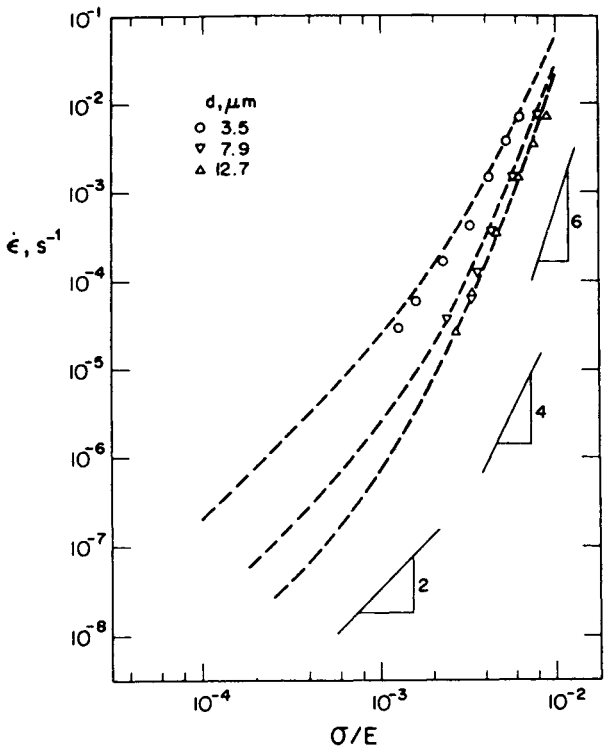

Fig. 4. The steady state creep rate as a function of the modulus-compensated stress for a fine-grained Cu-Al-Si-Co alloy at 500°C. o d=3.5 μm; ▽ d=7.9 μm; △ d=12.7 μm. The broken lines are predicted from Eq. (16) using $c_1 = 8.6 \times 10^{-16}$ $m^3 s^{-1}$, $c_2 = 4.4 \times 10^{-5}$ $m^3 s^{-1}$, $c_3 = 1.7 \times 10^{10}$ $m^3 s^{-1}$

data:

$$\dot{\varepsilon} = c_1/d^3 (\sigma/E)^2 + c_2/d^2 (\sigma/E)^4 + c_3 (\sigma/E)^6 \quad (16)$$

where c_1 is associated with D_{gb} (Eq. (6)), c_2 is associated with D_p (Eq. (11)) and c_3 is related to slip creep. The slip creep term is given as stress to the sixth power, which is near to that given by Eq. (12). It can be seen an excellent agreement between Eq. (16) and the experimental data.

In order to test the importance of pipe diffusion in the creep of fine-grained materials, the data of Shei and Langdon were analyzed by a traditional approach in which only the additive contributions of the normally accepted GBS term and the slip creep term were considered, i.e. Eq. (16) was used without the use of the pipe diffusion term. The resulting correlation is shown in Fig. 5. The predictive curves do not agree at all with the experimental data, indicating the necessity for including the pipe diffusion contribution.

Subgrain size

It is well established that subgrain boundaries are formed during creep flow of polycrystalline metals at elevated temperature. Furthermore, subgrains were shown to be a basic structural feature of steady state flow structures [67,68,78], with the subgrain size, λ, given by the relation:

$$\lambda = A_\lambda b (\sigma/E)^{-1} \quad (17)$$

where A_λ is about 4 for many materials.

Thus, the slip creep equation (Eq. (7)), which shows excellent correlations with experimental data, must take into consideration structure as a variable. It is, therefore, important to obtain a creep relation determined at constant structure in order to evaluate the possible influence of dislocation structure (i.e. subgrains) on the creep rate.

Constant structure creep tests were analyzed in order to studied the creep rate-stress relationship at constant subgrain size [79]. Such studies reveal that for a large number of materials $\dot{\varepsilon} \propto \lambda^3$. The introduction of a structure term in the slip creep relation (Eq. (7)), considering the strain rate dependence with subgrain size and Eq. (17), yields the following equation in the power law region of creep:

$$\dot{\varepsilon} = 10^9 (\lambda/b)^3 (D_L/b^2) (\sigma/E)^8 \quad (18)$$

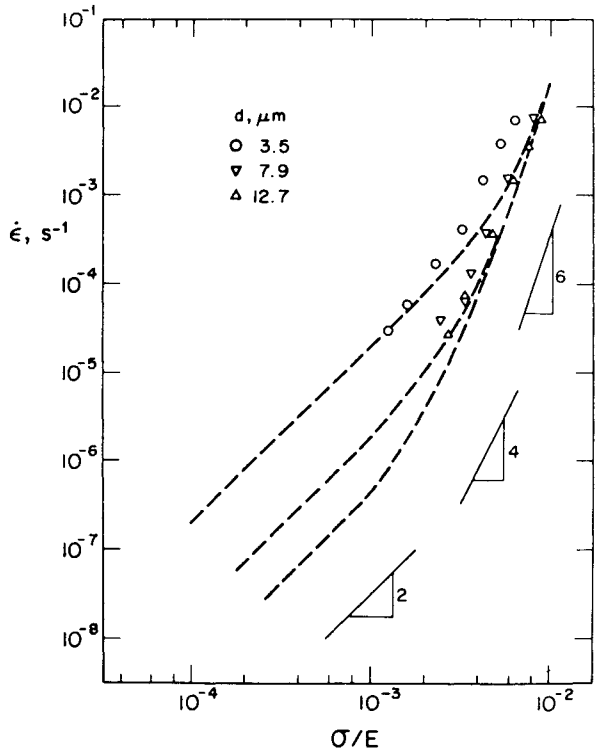

Fig. 5. The steady state creep rate as a function of the modulus-compensated stress for a fine-grained Cu-Al-Si-Co alloy at 500°C. ○ d=3.5 μm; ▽ d=7.9 μm; △ d=12.7 μm. The broken lines are predicted from Eq. (16) where the pipe diffusion term was neglected.

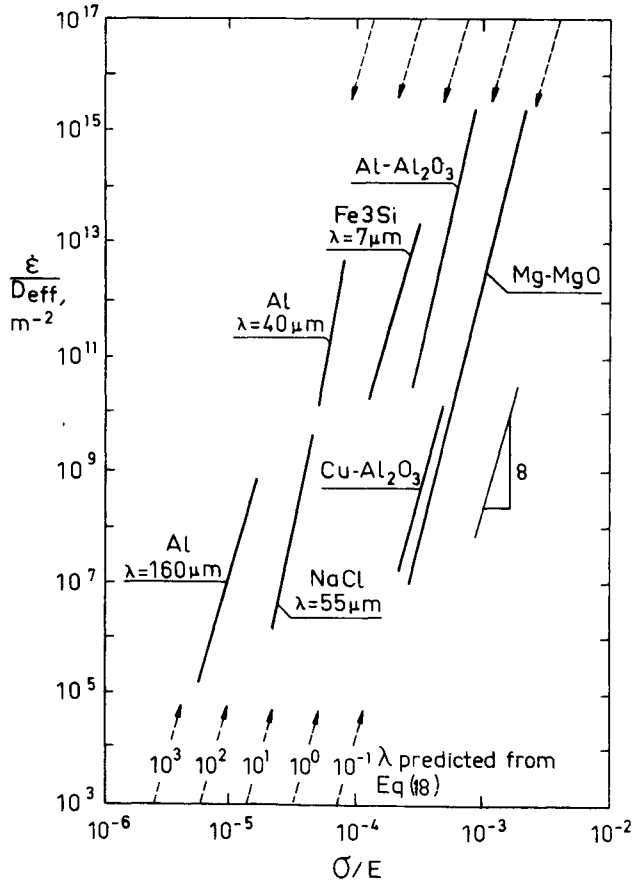

Fig. 6. Diffusion- compensated strain rate as a function of modulus- compensated stress for various materials. Al, Fe-3%Si and NaCl are tested under constant structure conditions.

This equation predicts that the creep rate will follow an eight power law relation if the structure is constant.

Many oxide dispersion strengthened (ODS) materials contain fine subgrain structures that are stabilized by the presence of the fine second phase oxide particles. Such ODS alloys are then likely candidates to exhibit invariant structures during creep deformation [80]. Figure 6 shows effective diffusion-compensated creep rate as a function of the modulus-compensated stress for some ODS materials as well as for Al, Fe-3Si and NaCl. The data for the latter three materials were obtained at a given subgrain size. The data for the ODS alloys were obtained under conditions of constant structure. The predicted curves from Eq. (18) as a function of subgrain size are given in the upper part of the figure. The data illustrate that the average stress exponent for creep is high and equal to about 9 which is close to predicted value of 8, and quite different from the value of 5 for pure metals. As shown, the experimental curves fit well the predicted lines, and confirm the important influence of subgrain size in describing the creep behavior over a wide range of strain rates.

Internal stresses; Harper-Dorn creep

It is well known that internal stresses can be generated in a material in a number of ways, most commonly by the presence of dislocations in the matrix. Quantitatively, it is difficult to calculate the true values of the internal stress through analytical methods and no successful attempts have been made to determine such stress.

High internal stress can arise from phase transformations involving volume changes from one phase to another phase, from grain shape mismatch during temperature change due to anisotropy of thermal expansion coefficients, and from the presence of defects by radiation damage. The presence of random dislocations can also contribute to the internal stress.

A phenomenological model that incorporates an internal stress term, σ_i, may be developed using Eq. (7) for slip creep [81]. The physical basis of the internal stresses is as follows: dislocations moving under an applied stress are envisioned to be both aided and inhibited by the presence of the internal stress fields that arise from stationary dislocations. Specifically, it can be considered that, at any given moment, one-half of the moving dislocations are influenced by an internal stress that adds to the applied stress and the remaining half of the moving dislocations are influenced by an internal stress that subtracts from the applied stress. This concept can be formulated by the equation:

$$\dot{\varepsilon} = 1/2\,\dot{\varepsilon}^*\,[f(\sigma+\sigma_i)] + 1/2\,\dot{\varepsilon}^*\,[f(\sigma-\sigma_i)] \qquad (19)$$

Using the slip creep equation (Eq. (7)) for the $\dot{\varepsilon}^*$ function of σ and σ_i, the following equation is obtained:

$$\dot{\varepsilon}=A_{pl}D_{eff}/2b^2[(\sigma+\sigma_i/E)^n + \frac{|\sigma-\sigma_i|}{(\sigma-\sigma_i)}(|\sigma-\sigma_i|/E)^n] \qquad (20)$$

where A_{pl} is the slip creep constant (power law).

If $\sigma_i \ll \sigma$, Eq. (20) reduces to the slip creep equation:

$$\dot{\varepsilon} = A_{pl}\,(D_{eff}/b^2)\,(\sigma/E)^n \qquad (21)$$

If $\sigma \ll \sigma_i$ then Eq. (20) reduces to a linear relation between $\dot{\varepsilon}$ and σ, yielding:

$$\dot{\varepsilon} = A_{pl}\,n\,(D_{eff}/b^2)\,(\sigma_i/E)^{n-1}\,\sigma/E \qquad (22)$$

This equation will be used to describe Harper-Dorn (H-D) creep based on the internal stress model.

Another equation that has been used to describe the uniaxial creep rate for H-D creep [72,82] is the following:

$$\dot{\varepsilon} = A_{HD}\,(D_L\,b/kT)\,\sigma \qquad (23)$$

where A_{HD} is a material constant.

Harper- Dorn creep data can be used to calculate the material constants A_{HD} (of Eq. (23)) and σ_i/E (of Eq. (22)). These constants are believed principally to be functions of the dislocation density and dislocation substructure [76].

An example of the predictive aspect of Eq. (20) is shown in Fig. 7 for pure aluminum using a value of $\sigma_i/E=2.5\times10^{-6}$. The figure illustrates that Newtonian viscous behavior is observed in the H-D region at stress values below about $\sigma/E = 3 \times 10^{-6}$; power law creep, with n = 5, is observed at stresses above about $\sigma/E = 3 \times 10^{-6}$. The solid line drawn through the data points is that obtained from Eq. (20) and provides strong support for the internal stress model. The value of internal stress is related to the dislocation density and can be calculated through the Taylor relation [83]. It will be shown later that this equation for describing H-D creep is applicable to a large number of pure metals studied at low stresses near the melting point.

There have been a remarkable revival of

interest in H-D creep in recent years and a further discussion of this subject will be presented in the last section of this paper.

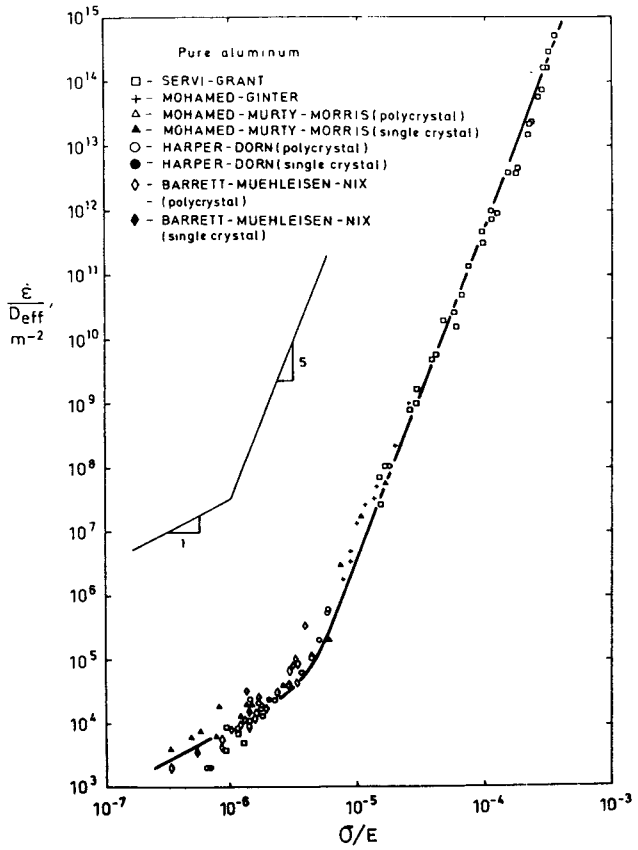

Fig. 7. Diffusion- compensated strain rate as a function of modulus- compensated stress for pure aluminum in the power law and Harper-Dorn creep regimes. The solid line is predicted from Eq. (20).

4. Competition between deformation mechanisms.

We have seen that a polycrystalline material can deform plastically in a number of ways each of which is described by a different deformation mechanism. Each mechanism is considered to operate independently of the others and has a particular dependence of creep rate with stress, temperature and grain size.

Over a certain temperature and strain rate range only one particular deformation mechanism will operate because, being independent, all mechanisms operate simultaneously and the faster will control creep.

It is usual in the literature to use only the equations of diffusional flow (Eqs. (3) and (4)) and slip (Eq. (7)) when considering the possible controlling mechanism for creep of polycrystalline materials at high temperature. It is our contention that grain boundary sliding, given by Eqs. (5) and (6), usually dominates the deformation process in the range where diffusional creep proceses are claimed to be rate-controlling. Examples are given in the following to present this view.

Creep data of β-Co was obtained by Sritharan and Jones [50] at various temperatures and grain sizes. These investigators suggested that the data can be explained by diffusional (Coble) creep accompanied by a threshold stress below which creep will not occur. The β-Co creep data at 773 K and 1073 K is plotted on a double-logarithmic scale in Fig. 8. The creep data at 1073 K do not seem to show evidence of a threshold stress. Rather, two linear regions are observed; the slope at low stresses is equal to about 2, a value that can be associated with GBS, and the slope at high stresses is about 4-5,

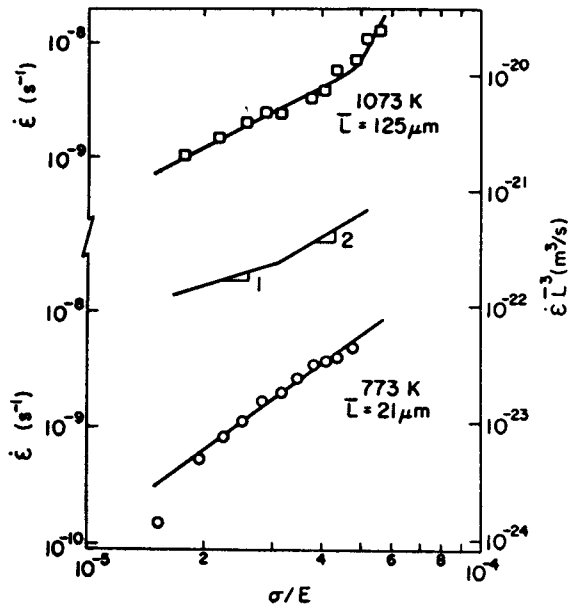

Fig. 8. Strain rate as a function of modulus- compensated stress for the creep of β-Co. The data were taken from reference 50.

which in turn can be associated with slip creep. The creep data at 773 K reveal a pattern that can be interpreted to show a threshold stress. If the lowest point is not considered, however, the remainder of the data can be accurately described by means of a straight line. The slope of this line is nearly equal to 2 and also suggests evidence for GBS as a deformation mechanism. The data of Fig. 8 can be analyzed in the light of predictions made by Eq. (6). If Eq. (6) is valid, the value obtained for the activation energy for creep should be related to the activation energy for grain boundary diffusion. Thus, a plot of $\dot{\varepsilon}d^3$ (or $\dot{\varepsilon}\bar{L}^3$) versus σ/E allows the activation energy for creep to be determined. The right-hand scale of Fig. 8 gives the values of $\dot{\varepsilon}\bar{L}^3$ for the two test temperatures, 773 K and 1073 K. An activation energy for creep of 130 kJ mol^{-1} is

obtained at $\sigma/E=4 \times 10^{-5}$. This value is nearly equal to the activation energy for grain boundary diffusion, $Q_{gb}=117$ kJ mol^{-1}, reported by Brik et al. [84].

Equations (4) and (6) were used to predict the creep rate of polycrystalline cobalt and the results of these predictions are shown in Fig. 9. In this figure the creep rate is normalized with respect to d and D_{gb}, and is plotted as a function of σ/E. As can be seen, the creep data follow closely the line predicted by the GBS equation, both in absolute values and in the slope. In contrast, the diffusional creep prediction falls below most of the data.

The conclusions described for β-Co were also verified for other metals. A way of illustrating this point is to prepare a Langdon-Mohamed deformation

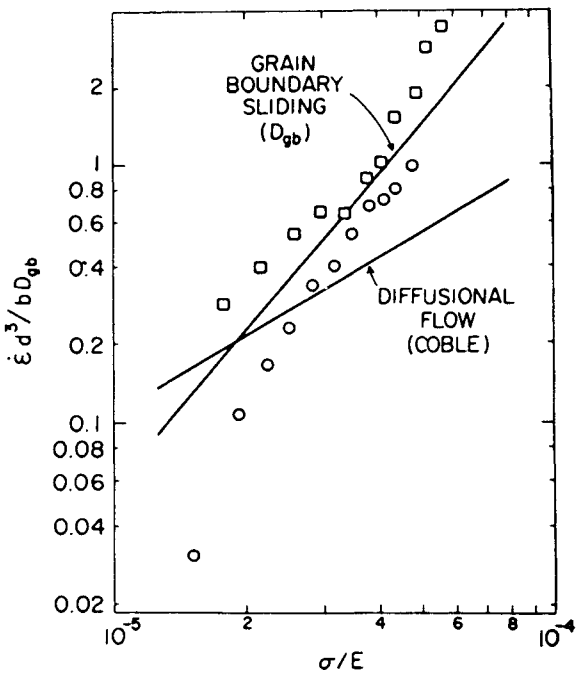

Fig. 9. Comparison of creep data for β-Co at 773 (○) and 1073 (□) with predictions from grain boundary sliding (D_{gb} controlled) and diffusional creep (Coble).

mechanism type of map [85,86]. This map predicts the deformation mechanisms expected at different grain sizes and modulus-compensated stresses. Figure 10 illustrates such a map at 0.55 T_m based on diffusional creep (Eqs. (3), (4) and (10)), GBS (Eqs. (5), (6) and (11)) and slip creep (Eqs. (7), (12) and (23)). The material constants used for the construction of this map are given in Table III. The values of modulus-compensated stress used in the creep tests for β-cobalt [50], α-iron [87], copper [88], magnesium [89] and 304 stainless steel [90] are plotted as a function of the grain size for those investigations where diffusional (Coble) creep with a threshold stress was believed to be operational. As

Table III. The material constants used for the construction of the deformation mechanism map shown in Fig. 10.

$A_{HD} = 1.7 \times 10^{-11}$
$E = 6.9 \times 10^{10}$ Pa
$b = 2.5 \times 10^{-10}$ m
$k = 1.38 \times 10^{-23}$ J K^{-1}
$T = 1000$ K
$D_{gb} = D_p = 2 \times 10^{-12}$ m^2 s^{-1}
$D_L = 10^{-19}$ m^2 s^{-1}

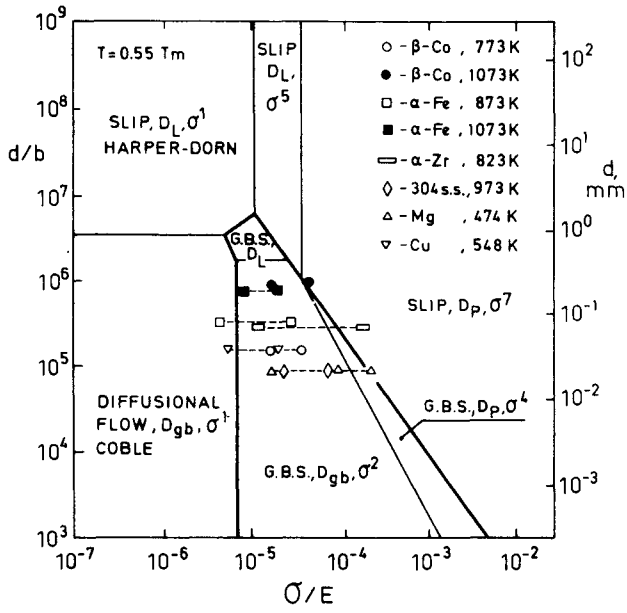

Fig.10. Deformation mechanism map at an homologous temperature $T/T_m=0.55$. The material constants used for the construction of the map are given in Table III.

can be seen, most of the data for those metals fall in the stress range where D_{gb}-controlled GBS dominates the deformation.

Another material analized was an austenitic stainless steel (25Cr- 20Ni) investigated by Yamane et al. [91]. These authors interpreted also their results by diffusional (Coble) creep and a threshold stress. They studied the influence of stress on the steady-state creep rate of antimony-addition stainless steels for a number of different grain sizes. Their data are plotted in Fig. 11 as grain size-compensated stress against the modulus-compensated stress. Predictions based on diffusional flow and on grain boundary sliding are given by the full lines shown in the figure. The predicted lines from Nabarro-Herring creep (Eq. (3)) and from Coble creep (Eq. (4)) are observed to result in creep rates that are considerably below the

experimental data. On the other hand, the predicted lines from the grain boundary sliding model (Eq. (5) and (11)) show excellent agreement with the data. The important feature of Fig. 11 is the transition from σ^2 to σ^4 behavior in agreement with a change from GBS (D_L) to GBS (D_p) behavior.

A deformation mechanism map at 0.7 T_m is constructed in Fig. 12. The relations used for the construction of the map are the same as for the map of Fig. 10. The material constants used are given in Table IV. The stress and grain size region covered by Yamane et al. is shown in the figure. As can be seen, deformation of the 25Cr-20Ni stainless steel in this range is predicted to be principally by grain boundary sliding and by slip creep. Only if GBS is ignored as a

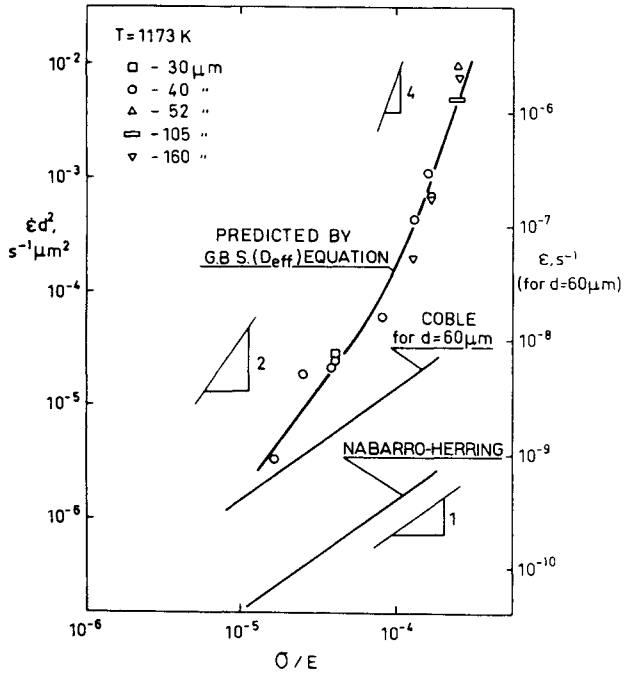

Fig. 11. The predicted grain-size- compensated strain rate-modulus- compensated stress relations for both grain boundary sliding and diffusional creep flow models are shown with experimental data for 25Cr-20Ni stainless steel from Yamane et al. [91].

Table IV. The material constants used for the construction of the deformation mechanism map shown in Fig. 12.

$A_{HD} = 1.7 \times 10^{-11}$
$E = 6.9 \times 10^{10}$ Pa
$b = 2.5 \times 10^{-10}$ m
$k = 1.38 \times 10^{-23}$ J K^{-1}
$T = 1173$ K
$D_{gb} = D_p = 9.8 \times 10^{-12}$ m^2 s^{-1}
$D_L = 1.68 \times 10^{-17}$ m^2 s^{-1}

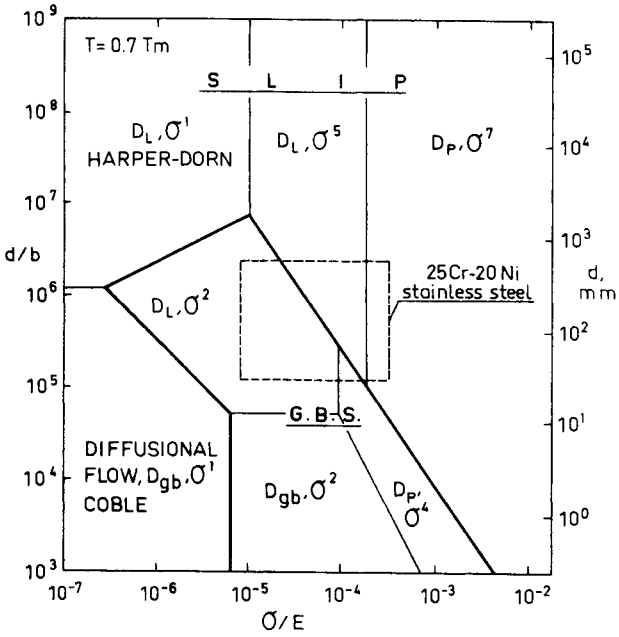

Fig.12. Deformation mechanism map at an homologous temperature T/T_m=0.7. The grain size and stress regimes used in the experimental study of Yamane et al. [91] are shown on the figure as the region bounded by broken lines. The material constants used for the construction of the map are given in Table IV.

mechanism does the diffusional creep regime become important. Therefore, using a deformation map that includes the important contributions of GBS mechanisms, Coble creep is predicted not to occur in the stress range investigated by Yamane et al. and only becomes important at fine grain sizes and at values of σ/E below 3×10^{-6}.

The examples given above indicate the importance of grain boundary sliding as a mechanism at low stresses and intermediate temperatures. Creep at low stresses and high temperatures, however, is often controlled by either Nabarro-Herring diffusional creep, grain boundary sliding or Harper-Dorn creep. Recents investigations on H-D creep [92-97], in fact, suggest that this mechanism is more important than normally considered. A summary of this study is given in the following paragraph.

There are a large number of studies covering the deformation of a large number of polycrystalline metals at low stresses and high temperatures [98]. In these studies, a linear dependence of strain rate with stress was also reported, and Nabarro-Herring diffusional creep was described as the mechanism of plastic flow. Figure 13 show the ratio of the diffusion coefficient estimated from creep, D_{creep}, to the radiotracer diffusion value, D_{exp}, plotted as a function of a dimensionless test duration parameter $P = (D_{exp} t/a^2)^{1/2}$, where t= test time and a=

product of the grain dimensions, and is taken from the work of Jones [98]. As can be observed from the figure, the creep rates of most of these metals (i.e. γ-Fe [99], Ni [100], Ag [101], β-Co [102], Cu [103], Mo [104] and Cr [104]), however, are significantly faster than those predicted by the diffusional (Nabarro-Herring) creep relation. These high rates were attributed to a transient effect from dislocation short-circuiting during diffusional creep.

Another possible explanation for the observed high creep rates in this group of metals is that H-D diffusion-controlled-dislocation creep takes place more readily than diffusional creep.

A deformation mechanism map was constructed for analyses of those metals that exhibit anomalous diffusional creep behavior. Figure 14 shows a plot

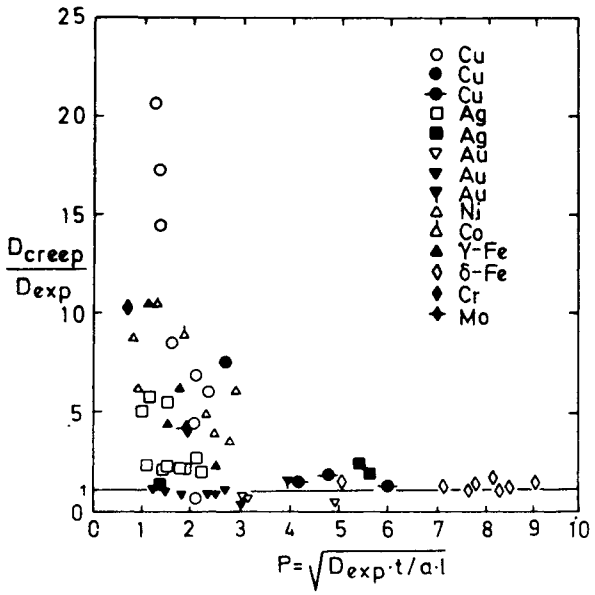

Fig. 13. The ratio of the diffusion coefficient estimated from creep D_{creep} to the diffusion coefficient experimentally determined by radiotracer analysis D_{exp} as a function of a dimensionless test duration parameter $P = (D_{exp} \cdot t)/a \cdot l)^{1/2}$ for various pure metals. Taken from reference [98].

Table V. The material constants used for the construction of the deformation mechanism map shown in Fig. 14.

$A_{HD} = 1.5 \times 10^{-10}$
$E = 9 \times 10^{10}$ Pa
$b = 2.6 \times 10^{-10}$ m
$k = 1.38 \times 10^{-23}$ J K^{-1}
$T = 1600$ K
$D_{gb} = D_p = 1.5 \times 10^{-10}$ m^2 s^{-1}
$D_L = 2 \times 10^{-13}$ m^2 s^{-1}

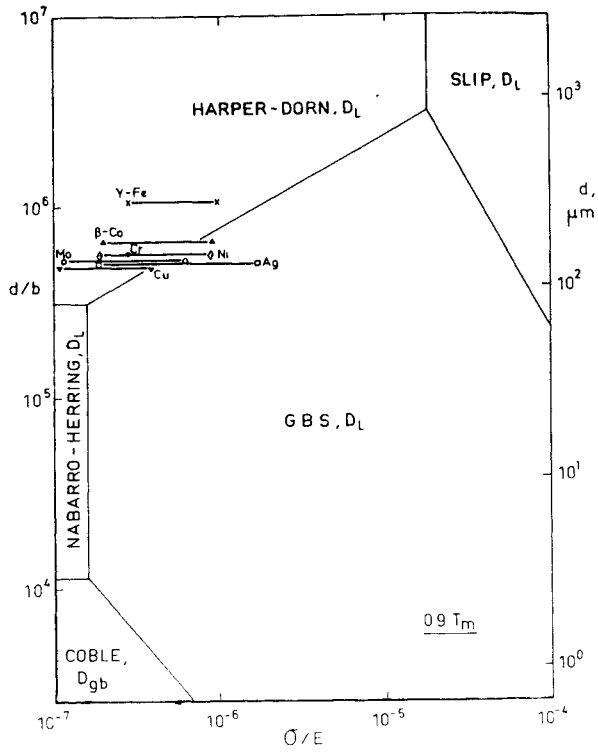

Fig. 14. Deformation mechanism map at an homologous temperature $T/T_m=0.9$ showing location of metals exhibiting anomalous diffusional creep behavior. The material constants used for the construction of the map are given in Table V.

of grain-size normalized by the Burgers' vector, d/b, as a function of the modulus-compensated stress, σ/E, at a homologous temperature of 0.90 T_m. The relations used for the construction of the map are the same as for the other maps. The material constants used are given in Table V. A value of A_{HD} equal to 1.5×10^{-10} was used. This is the expected value for H-D creep at 0.9 T_m where most of the creep tests were carried out. The map of Fig. 14 shows the range of stresses used in the low stres creep studies on metals that exhibit anomalously high diffusional-flow creep rates. The lines all fall in the H-D region at low stresses, and in a GBS region at high stresses. It is clear from the deformation map that Nabarro-Herring creep will only be rate controlling for these metals at grain sizes less than 100 μm and at stresses less than 2×10^{-7} E.

References

[1] Seeger A., Diehl S., Mader S., Rebstock H., Philos. Mag. 2(1957)323.
[2] Friedel J., *Dislocations* (Oxford, Pergamon Press) 1964, p.491.
[3] Mott N.F., Philos. Mag. 44(1953)742.
[4] Conrad H., J. Met. 16(1964)582.
[5] Escaig B., J. Physique 28(1967)171.
[6] Robinson S.L., Sherby O.D., Acta Metall., 17(1969)109.

[7] Ruano O.A., Miller A.K., Sherby O.D., Mater. Sci. Eng. 51(1981)9.
[8] Nabarro F.R.N., Rep. Conf. on the Strength of Solids (London, Physical Society)1948, p.75.
[9] Herring C., J. Appl. Phys. 21(1950)437.
[10] Coble R.L., J. Appl. Phys. 34(1963)1679.
[11] Geckinli A.E., Barrett C.R., J. Mater. Sci. 11(1976)510.
[12] Ashby M., Verrall R., Acta Metall. 21(1973)149.
[13] Ball A., Hutchison M.M., Mater. Sci. J. 3(1969)1.
[14] Mukherjee A.K., Mater. Sci. Eng. 8(1971)83.
[15] Gifkins R.C., Metall. Trans. 7A(1976)1225.
[16] Langdon T.G., Philos. Mag. 22(1970)689.
[17] Gittus J.H., Trans. ASME, J. Eng. Mater. Technol. 99(1977)244.
[18] Hayden H.W., Floreen S., Goodell P.D., Metall. Trans. 3(1972)833.
[19] Arieli A., Mukherjee A.K., Mater. Sci. Eng. 45(1980)61.
[20] Padmanabhan K.A., Mater. Sci. Eng. 40(1979)285.
[21] White R.A., Ph.D. Thesis, Department of Materials Science and Eng., Stanford University (1978).
[22] Sherby O.D., Ruano O.A., *Superplastic Forming of Structural Alloys*, Eds. Paton N.A., Hamilton C.H. (New York, TMS-AIME) 1982, p.241.
[23] Naziri H., Pearce R., Brown M., Hale K.F., Acta Metall.
[24] Holt D.H., Trans. AIME 242(1968)25.
[25] Alden T.H., Schadler H. W., Trans. AIME 242(1968)825.
[26] Franti G.W., Wilsdorf H.G.F. , Rep. MS-3557-102-75, University of Virginia (1975)
[27] Mohamed F.A., Shei S., Langdon T.G. , Acta Metall. 23(1975)1443.
[28] Yaidya M.L., Murty K.L.,Dorn J.E., Acta Metall. 21(1973)1615.
[29] Packer C.M., Ph.D. Thesis, Department of Materials Science and Eng., Stanford University (1967).
[30] Naziri H., Pearce R., J. Inst. Met. 101(1973)197.
[31] Kossowski R., Bechtold J.H. , Trans. AIME 242(1968)716.
[32] Prematta R.J., Yenkatesan P.S., Pense A., Metall. Trans. 7A(1976)1235.
[33] Schadler H.W., Trans. AIME 242(1968)1281.
[34] Morrison W.B., Trans. ASM 61(1968)923.
[35] Mohamed F.A., Langdon T.G., Philos. Mag. 32(1975)697.
[36] Cline H.E., Alden T.H., Trans. AIME 239(1967)710.
[37] Zehr S.W., Backofen W.A., Trans. ASM 61(1968)300.
[38] Alden T.H., Trans. ASM 61(1968)559.
[39] Chaudari P., Mader S., Proc. 7th Int.Conf on High Speed Testing; in Appl. Polym. Symp. 12(1969)1.
[40] Kayali E.S., Ph.D. Thesis, Department of Materials Science and Eng., Stanford University (1967).
[41] Alden T.H., Trans. AIME 236(1966)1633.
[42] Alden T.H., Acta Metall. 15(1967)469.
[43] Sherby O.D., Walser B., Young C.M., Cady E.M., Scripta Metall. 9(1975)569.
[44] Clark M.A., Alden T.H., Acta Metall. 12(1973)1195.
[45] Naziri N., Pearce R., J. Inst. Met. 98(1970)71.
[46] Lee J.D., Niessen P., Metall. Trans. 4(1973)949.
[47] Melton K.N., Edington J.W., Scripta Metall. 9(1975)559.
[48] Bly D.L., Ph.D. Thesis, Department of Materials Science and Eng., Stanford University (1973).
[49] Every D.H., Backofen W.A., Trans. ASM 58(1965)551.
[50] Sritharan T., Jones H., Acta Metall. 27(1979)1293.
[51] Stowell M.J., Robertson J.L., Watts B.M., Met. Sci. J. 3(1969)41.
[52] Herriot G., Suery M., Baudelet B., Scripta Metall. 6(1972)657.
[53] Watts B.M., Stowell M.J., Baikie B.L., Owen D.G.E., Met. Sci. J. 10(1976)189.
[54] Segat B., Blenkinsop P., Taplin D.M.R., J. Inst. Met. 100(1972)268.
[55] Holt D.H., Backofen W.A., Trans. ASM 59(1966)755.
[56] Rai G., Grant N.J., Metall. Trans. 6A(1975)385.
[57] Dunlop G.L., Shapiro E., Taplin D.M.R., Crane J., Metall. Trans. 4(1973)2039.
[58] Weinstein D., Trans. AIME 245(1969)2041.
[59] Lee D., Acta Metall. 17(1969)1057.
[60] Lee D., Backofen W.A., Trans. AIME 239(1967)1034.
[61] Cline H.E., Trans. AIME 239(1967)1906.
[62] Smith C.I., Norgate B., Ridley N., Met. Sci. J. 10(1976)182.
[63] Karim A., Backofen W.A., Metall. Trans. 3(1972)709.
[64] Hayden H.W., Gibson R.C., Merrick H.F., Brophy J.H., Trans. ASM 60(1967)3.
[65] Cline H.E., Lee D., Acta Metall. 18(1970)315.
[66] Dorn J.E., *Creep and Fracture of Metals at High Temperature*, (London, H.M. Stationery Office) 1957, p.89.
[67] Sherby O.D., Burke P.M., Progr. Mater. Sci. 13(1968)325.
[68] Bird J.E., Mukherjee A.K., Dorn J.E., Int. Conf. Quantitative Relation Between Properties and Microstructure, Haifa, Israel (1969) p. 255.
[69] Weertman J., Trans. ASM 61(1968)681.
[70] Weertman J., J. Appl. Phys. 28(1957)362.
[71] Barrett C.R., Nix W.D., Acta Metall. 13(1965)1247.
[72] Harper J.C., Dorn J.E., Acta Metall. 5(1957)654.
[73] Spingarn J.R., Barnett D.M., Nix W.D., Acta Metall. 27(1979)549.
[74] Luthy H., Miller A.K., Sherby O.D., Acta Metall. 28(1980)169.
[75] Frost H.J., Ashby M.F., *Deformation-Mechanism Maps* (Pergamon Press) 1982.
[76] Garofalo F., Domis W.D., von Gemmingen F., Trans. AIME 230(1964)1460.
[77] Shei S.A., Langdon T.G., Acta Metall. 26(1978)639.
[78] Weertman J., Trans. ASM 61(1968)681.
[79] Sherby O.D., Klundt R.H., Miller A.K., Metall. Trans. 8A(1977)843.
[80] Lin J., Sherby O.D., Res Mechanica 2(1981)251.
[81] Wu M.Y., Sherby O.D., Acta Metall. 32(1984)1561.
[82] Langdon T.G., Yavari P., Acta Metall. 30(1982)881.
[83] Ruano O.A., Wadsworth J., Sherby O.D., submitted to Acta Metall.
[84] Brik Y.B.,Larikov L.N., Falchenko Y., Ukr. Fiz. Zh. (Ukr. Edn.), 20(1975)397.
[85] Langdon T.G., Mohamed F.A., Mater. Sci. Eng. 32(1978)103.
[86] Mohamed F.A., Langdon T.G., Metall. Trans. 5(1974)2339.
[87] Towle D.J., Jones H., Acta Metall. 24(1976)399.
[88] Crossland I.G., *Physical Metallurgy of Reactor Fuel Elements*, Eds. Harris J.E., Sykes E.C., (London, Metals Society) 1975, p.66.
[89] Crossland I.G., Jones R.B., Met. Sci. 11(1977)504.
[90] Sritharan T., Jones H., Acta Metall. 28(1980)1633.
[91] Yamane T., Gemna N., Takahashi Y., J. Mater. Sci. 19(1984)263.
[92] Mohamed F.A., Ginter T.G., Acta Metall. 30(1982)1869.
[93] Ginter T.J., Mohamed F.A., J. Mater. Sci. 17(1982)2007.
[94] Langdon T.G., Yavari P., Acta Metall. 30(1982)881.
[95] Weertman J., Blacic J., Geophys. Res. Lett. 11(1984)117.
[96] Raj S.Y., Scripta Metall. 19(1985)1069.
[97] Ardell A.J., Lee S.S., Acta Metall. 34(1986)2411.
[98] Jones H., Mater. Sci. Eng. 4(1969)106.
[99] Price A.T., Holl H.A., Greenough A.P., Acta Metall. 12(1964)49.
[100] Hayward E.R., Greenough A.P., Mater. Sci. Eng. 4(1969)106.
[101] Funk E.R., Udin H., Wulff J., Trans. AIME 191(1951)206.
[102] Bryant L.F., Speiser R. Hirth J.P., Trans. AIME 242(1968)1145.
[103] Udin H., Shaler A.J., Wulff J., Trans. AIME 185(1949)186.
[104] Allen B.C., Trans. AIME 236(1966)903.